

# **Electrochemical Aqueous Sodium Chloride Solutions (Anolyte and Catholyte) as Types of Water. Mathematical Models. Study of the Effects of Anolyte on the Virus of Classical Swine Fever Virus.**

Ignat Ignatov<sup>1\*</sup> Stoil Karadzhov<sup>2</sup> Atanas Atanasov<sup>3</sup> Emiliya Ivanova<sup>4</sup> Oleg Mosin<sup>5</sup>

1. DSc, Professor, Scientific Research Center of Medical Biophysics (SRCMB),

N. Kopernik Street, 32, Sofia 1111, Bulgaria

2.DSc., Professor, Bulgarian Association of Activated Water, Kutuzov blvd, 39, 1619 Sofia, Bulgaria

3. Eng., Bulgarian Association of Activated Water, Kutuzov blvd, 39, 1619 Sofia, Bulgaria

4. PhD, Ass. Prof., National Diagnostic and Research Veterinary Medical Institute "Prof. Dr. Georgi Pavlov", P. Slaveykov, 16, 1606 Sofia, Bulgaria

5. PhD (Chemistry), Ass. Prof., Biotechnology Department, Moscow State University of Applied Biotechnology,

Talalikhina Street, 33, Moscow 109316, Russian Federation

\* E-mail of the corresponding author: mbioph@dir.bg

## **Abstract**

The results of antimicrobial action of an acid (anolyte) solution in electrochemical activation of sodium chloride are provided. Mathematical models are made of an acid (anolyte) and alkaline (catholyte) solution in electrochemical activation of sodium chloride. Anolyte water is produced by electrolyzing salt in the anode chamber of an electrolytic cell. Catholyte water is produced by electrolyzing water in the anode chamber of an electrolytic cell. Under laboratory conditions cell culture and organ suspensions of Classical swine fever virus were treated with anolyte. By inoculating them with cell cultures quality (displayed) viral presence (presence of viral antigen) was reported using the immunoperoxidase technique. It was found that: anolyte did not affect the growth of the cell culture PK-15; viral growth in the infection of a cell monolayer with a cell culture virus was affected in the greatest degree by anolyte in 1:1 dilution and less by the other dilutions; viral growth in the infection of a cell suspension with cell culture virus was affected by anolyte in dilution 1:1 in the greatest degree, and less by the other dilutions; viral growth in the infection with a virus in organ suspension of a cell monolayer was affected by the anolyte in all dilutions applied.

In order to provide additional information about the antiviral activity of anolyte, and about the distribution of water molecules according to the energies of the hydrogen bonds, mathematical models are made of anolyte and catholyte (Ignatov, Mosin, 2013).

This review reports about the research on the structure of intermolecular water cyclic associates (clusters) with general formula  $(\text{H}_2\text{O})_n$  and their charged ionic clusters  $[\text{H}^+(\text{H}_2\text{O})_n]^+$  and  $[\text{OH}^-(\text{H}_2\text{O})_n]^-$  by means of computer modeling and spectroscopy methods as  $^1\text{H}$ -NMR, IR-spectroscopy, DNES, EXAFS-spectroscopy, X-Ray and neutrons diffraction. Computer calculation of polyhedral nanoclusters  $(\text{H}_2\text{O})_n$ , where  $n = 3-20$  is carried out. Based on this data, the main structural mathematical models describing water structure (quasicrystalline, continuous, fractal, fractal-clathrate) were examined and some important physical characteristics were obtained. The average energy of hydrogen bonding among  $\text{H}_2\text{O}$  molecules in the process of cluster formation was measured by the DNES method compiles  $-0.1067 \pm 0.0011$  eV. It was also shown that water clusters formed from  $\text{D}_2\text{O}$  were more stable, than the ones from  $\text{H}_2\text{O}$  due to isotopic effects of deuterium. The distribution according to energies of the hydrogen bonds in anolyte and catholyte as a percentage of the molecules with a certain value of hydrogen bonds to the total amount. The measurement of  $(-E)$  is in the range of 0.08 to 0.14 eV.

**Keywords:** anolyte, cell culture, CSF virus, disinfection, hydrogen bond, water, structure, clusters.

## 1. Introduction

Water with its anomalous physical and chemical properties outranks all other natural substances on Earth. The ancient philosophers considered water as the most important component of matter. It performs a vital role in numerous biochemical and metabolic processes occurring in cells with participation of water, being a universal polar solvent for hydrophilic molecules having an affinity for water. Hydroxyl groups ( $-\text{OH}$ ) in  $\text{H}_2\text{O}$  molecule, are polar and therefore hydrophilic. Moreover water acts as a reagent for a big number of chemical reactions (hydrolysis, oxidation-reduction reactions). In chemical processes water, due to its high ionizing ability, possesses strong amphoteric properties, and can act both as an acid and a base in reactions of chemical exchange.

Modern science has confirmed the role of water as a universal life sustaining component, which defines the structure and properties of inorganic and organic objects consisting of water. The recent development of molecular and structural-chemical concepts has enabled to clarify an explanation of the ability of water molecules to form short-lived hydrogen bonds with neighboring molecules and many other chemical substances and to bond them into intermolecular associates. The role of bounded water in forming hydrated substances and their physicochemical conduct in aqueous solutions has also become clear.

Of great scientific and practical interest are the studies of a variety of specific supramolecular structures – cyclic water clusters described by general formula  $(\text{H}_2\text{O})_n$ , which may be calculated and studied with the help of modern numerical computing methods. The clusters are also important for studying the structure of water and hydration phenomena at a molecular level since they form the basic building blocks of the hydrated substances. This paper deals with the mathematical modeling of the water structure and water associates.

A current trend in the development of modern science and practice of disinfection is not the creation of new disinfectants but the search of methods to enhance the antimicrobial activity in order to reduce or completely eliminate the adverse effects on humans, animals, the environment, and to expand the range of action of the existing ones. In full accordance with this trend is the electrochemical activation of aqueous solutions with low mineralization, and especially aqueous solutions of sodium chloride to a concentration of 0.5%. By applying modern nanotechnology, disinfectants (anolyte) with outstanding antimicrobial

activity will be received by electrochemical activation. It is based on the nascent oxygen, chlorine dioxide, hydrogen peroxide, ozone and others contained therein. Nascent oxygen is produced only in the reaction mixture and it reacts at once with the reducing agent. Along with that, the electrochemically obtained disinfectants are distinguished by their full safety for humans, animals and the environment as they rapidly decompose to water and trace amounts of sodium chloride.

To study the antimicrobial effect of anolyte a number of experiments have been performed, the major part of them being aimed at determining its action on different types of bacteria. Studies in terms of its virucidal effect are few and of insufficient depth, making research on the possibilities of applying anolyte in the implementation of effective control of viral diseases in humans and animals and especially on particularly dangerous viral infections highly relevant. One of them is the classical swine fever, which is prevalent in different regions of the world, inflicting heavy economic losses. It is caused by enveloped viruses belonging to the genus Pestivirus of the family Flaviviridae. The resistance and inactivation of the virus of CSF virus are subject of extensive research. Although it is less resistant to external stresses other than the non-enveloped viruses, it retains for a long period of time its virulence: in frozen meat and organs – from a few months up to one year; in salted meat – up to three years; in dried body fluids and excreta – from 7 to 20 days. In rotting organs it dies for a few days, and in urine and faeces – for about 1-2 days. In liquid fertilizer it can withstand 2 weeks at 20 °C, and over 6 weeks at 4 °C. Its thermal resistance may vary depending on the strain, but the inactivation is dependent mostly on the medium containing the virus. Although the CSF virus loses its infectivity in cell cultures at 60 °C for 10 minutes, it is able to withstand at least 30 minutes at 68 °C in defibrinated blood. It is relatively stable at pH 5-10, and the dynamic of the inactivating process below pH 5 depends on the temperature.

According to Linton et al., (1987), Sands et al., (1979) and Springthorpe et al., (1990), effective disinfection with viruses whose infectivity is associated with the elements of the casing is achieved by disinfectants dissolving fats, surfactants, disinfectants or fatty acids, organic solvents (ether and chloroform), detergents, proteases, and common disinfectants. It is still believed that a 2% solution of sodium hydroxide is most suitable for the disinfection of spaces contaminated with them. According to Wittmann (1967), to achieve effective disinfection it is necessary to irreversibly damage their nucleic acid. The purpose of this study is to establish the virucidal effect of anolyte in different dilutions on Classical swine fever virus in cell culture and organ suspensions. Dependence is sought between the resulting local maximum at -0.1312 eV in the spectrum of anolyte and antiviral activity. At -0.1387 a local maximum is obtained in the catholyte solution which corresponds to inhibiting the development of tumor cells on a molecular level (Ignatov & Mosin, 2014). Effects of inhibiting the development of tumor cells on a molecular level are described in solutions with shungites and zeolite. Maximum effect is observed from a mixture of zeolite and shungites (Ignatov & Mosin, 2014).

## 2. Materials and methods

Fig. 1 demonstrates a laboratory setting for a membrane electrolysis method for the preparation of an acid (anolyte) and alkali (catholyte) solution in electrochemical activation of sodium chloride.

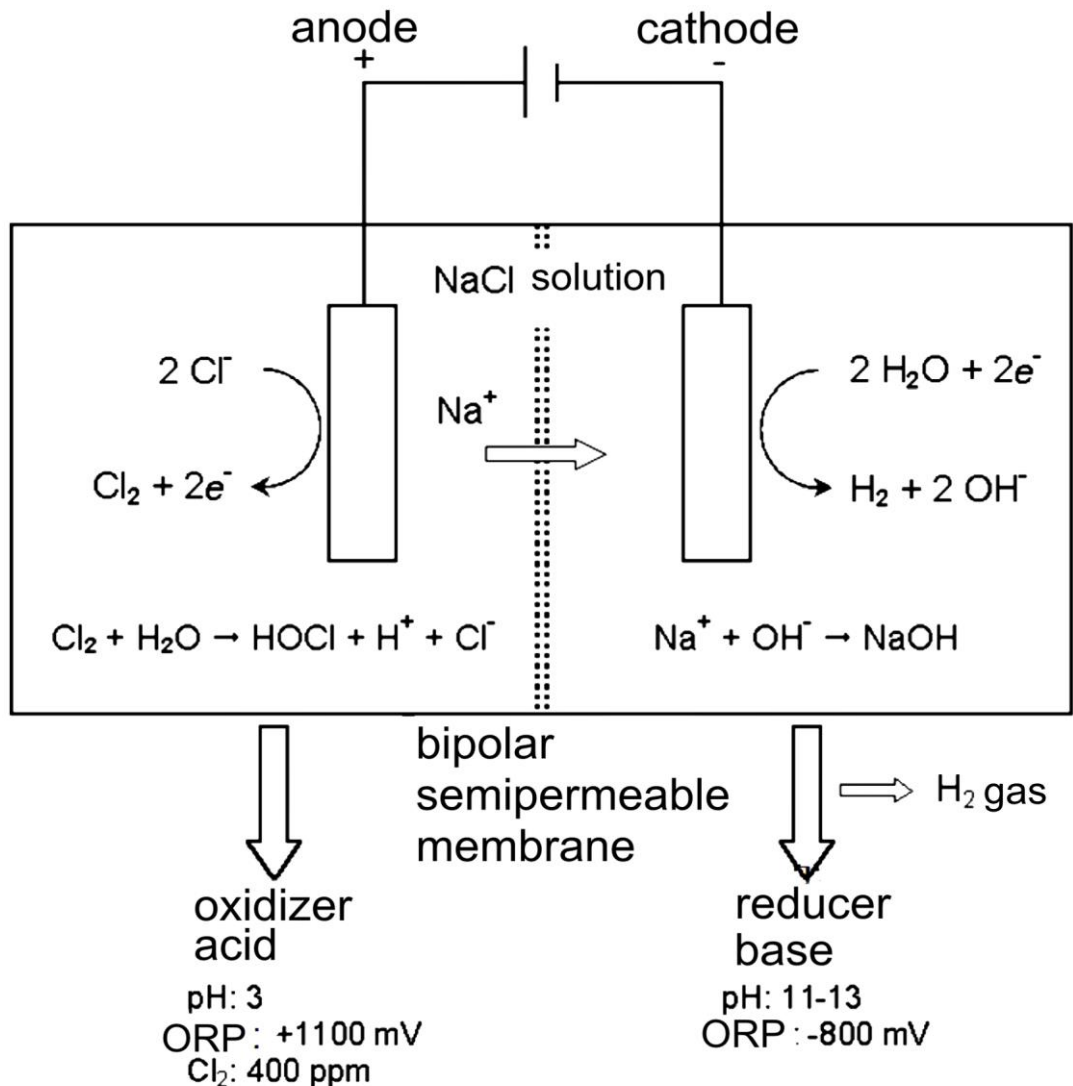


Figure 1. Laboratory setting for a membrane electrolysis method for the preparation of an acid (anolyte) and alkali (catholyte) solution in electrochemical activation of sodium chloride

Cluster structures in anolyte and catholyte are a private case of the cluster structures in water; they are calculated theoretically and are confirmed by computer through the following methods: <sup>1</sup>H-NMR, IR, Raman, Compton scattering, EXAFS-spectroscopy and X-ray diffraction (Ignatov, 2005; Mosin & Ignatov, 2011). Information obtained using the modern detection methods corresponds to femtosecond time, i.e. instantaneous dynamics of intermolecular interactions in the molecular scale. The presence of hydrogen bonding causes the noticeable effect on vibrational and <sup>1</sup>H-NMR spectra. In <sup>1</sup>H-NMR the chemical shift of the proton involved in the hydrogen bonding shifts about 0.01 ppm reducing strength of hydrogen bonding while the temperature is raised (Yamaguchi et al., 2001). Increased extent of hydrogen bonding within clusters results in a similar effect; the stronger the chemical shifts with greater connectivity, the shorter the

hydrogen bonded O-H...O distances.  $^1\text{H}$  peaks shift to greater ppm with the increase of hydrogen bonding strength.

In IR-spectroscopy the characteristic vibration frequency bands containing hydrogen are reduced in spectra if a hydrogen atom is included in the hydrogen bonding. Infrared absorption bands, such as OH-groups are much expanded when the hydrogen bond is formed, and their intensity increases. The main stretching band in liquid water is shifted to a lower frequency ( $\nu_3$ ,  $3480\text{ cm}^{-1}$  and  $\nu_1$ ,  $3270\text{ cm}^{-1}$ ), while the bending frequency ( $\nu_2$ ,  $1640\text{ cm}^{-1}$ ) increases with hydrogen bonding (Ohno *et al.*, 2005). Increased strength of hydrogen bonding shifts the stretch vibration to lower frequencies with greatly increased intensity in the infrared due to the increased dipoles. With the raising of the temperature the stretch vibrations shift to higher frequency, while the intramolecular vibrations shift to lower frequencies (Ignatov & Mosin, 2013b). Hydrogen bond energy lies in the range of 2.3 kcal/mole for the N-H...O-bonds up to 7.0 kcal/mol for the bonds with hydrogen fluoride F-H...F. The strength of the hydrogen bonding depends on the cooperative/anticooperative character of the surrounding hydrogen bonds with the strongest hydrogen bonds giving the lowest vibrational frequencies.

In X-ray absorption spectroscopy (EXAFS-spectroscopy) X-ray radiation excites the electrons of the inner shell of an oxygen atom in  $\text{H}_2\text{O}$  molecules and stipulates their transition onto unoccupied upper electronic levels in the molecules (Wernet *et al.*, 2004). Probability of electron transitions and characteristics of the absorption contour depends mostly on the molecular environment. This allows by varying the energy of the X-rays to study the distribution of associations for HOH...OH<sub>2</sub> bond judging on lengths and angles of the covalently bonded hydrogen atom in the molecule. EXAFS spectrum near the oxygen atom is also sensitive to hydrogen bonding. This method is used to obtain information about the molecular structure of water in the first coordination sphere. Since the time of excitation of electrons is much smaller than the vibrational motions in liquids, X-ray probe of the electronic structure provides information about the instantaneous changes of configurations of the water structure.

Diffraction techniques (X-ray and neutron diffraction) on liquid water allow to calculate the function of density radial distribution (O or H) and the probability of detection of  $\text{H}_2\text{O}$  molecules at a certain distance from a randomly chosen individual  $\text{H}_2\text{O}$  molecule (Tokushima *et al.*, 2008). This allows to detect the irregularities in water by constructing the radial distribution function, i.e. the distance between the atoms of O, H, and O-H in  $\text{H}_2\text{O}$  molecule and its nearest neighbors. Thus, the distribution of the distances between the oxygen atoms at a room temperature, gives three major peaks measured at 2.8, 4.5 and 6,7 Å. The first maximum corresponds to the distance to the nearest neighbor and its value is approximately equal to the length of the hydrogen bond. The second maximum is close to the average edge length of a tetrahedron, as  $\text{H}_2\text{O}$  molecules in the crystalline structure of ice  $\text{I}_h$  arranged at the vertices of the tetrahedron allocated around the center of the molecule. The third peak, expressed very weakly, corresponds to the distance to the third and more distant neighboring  $\text{H}_2\text{O}$  molecules on the hydrogen network. In 1970 I.S. Andrianov and I.Z. Fisher calculated the distance up to the eighth of the neighboring  $\text{H}_2\text{O}$  molecule; the distance to the fifth of the neighboring  $\text{H}_2\text{O}$  molecule turned out to be 3 Å, and to the sixth molecule – 3,1 Å. This allowed to draw conclusions about the geometry of hydrogen bonds and farther surroundings of  $\text{H}_2\text{O}$  molecules.

Another method for structural studies – neutron diffraction is similar to X-ray diffraction. However, because the neutron scattering lengths vary slightly among different atoms, this method is limited in the

case of the isomorphous substitution of hydrogen atoms in H<sub>2</sub>O molecule by deuterium (D). In order to structure theoretically the water molecules into crystals, by using mathematical approximation, other methods are employed. Then the intensity of the neutron diffraction of this crystal is measured. From these results, the Fourier transform is carried out; the measured neutron intensity and phase are being used for calculation. Then, on the resultant Fourier map hydrogen and deuterium atoms are represented with much greater atomic weight than on the electron density map, as the contribution of these atoms in neutron scattering is essentially big. On the resulting density map is determined the arrangement of hydrogen <sup>1</sup>H (negative density) and deuterium D (positive density) atoms. A variation of the method which describes that the crystal of an ordinary protonated water (H<sub>2</sub>O) before measurements is kept in 99.9 at.% of heavy water (D<sub>2</sub>O). In this case the neutron diffraction can not only establish the localization of the hydrogen atoms, but can also identify those protons that can be exchanged by deuterium, that is particularly important for the study of isotopic (H–D) exchange. Such information in some cases may help confirm the correctness of the water structure established by other methods.

Clusters formed of D<sub>2</sub>O are more stable and resistant than those from H<sub>2</sub>O due to isotopic effects of deuterium caused by 2-fold increasing nuclear mass of deuterium (molecular mass of D<sub>2</sub>O is more by 11% than that of H<sub>2</sub>O). The structure of D<sub>2</sub>O molecule is the same, as that of H<sub>2</sub>O, with small distinction in values of lengths of covalent bonds. D<sub>2</sub>O crystals have the same structure as a conventional ice I<sub>h</sub>, the difference in unit cell size is very insignificant (0.1%). But they are heavy (0.982 g/cm<sup>3</sup> at 0<sup>0</sup>C over 0.917 g/cm<sup>3</sup> for conventional ice). D<sub>2</sub>O boils at 101.44 <sup>0</sup>C, freezes at 3,82<sup>0</sup>C, has density at 20<sup>0</sup>C 1.105 g/cm<sup>3</sup>, and the maximum density occurs not at the 3.89<sup>0</sup>C, as for H<sub>2</sub>O, but at 11.2<sup>0</sup>C (1.106 g/cm<sup>3</sup>). The mobility of D<sub>3</sub>O<sup>+</sup> ion on 28.5% lower than that of H<sub>3</sub>O<sup>+</sup> ion and OD<sup>-</sup> ion – 39.8% lower than that of OH<sup>-</sup> ion, the constant of ionization of D<sub>2</sub>O is less than the constant of ionization of H<sub>2</sub>O, which means that D<sub>2</sub>O has a bit more hydrophobic properties than H<sub>2</sub>O. All these effects lead to the fact that the hydrogen bonds formed by deuterium atoms differ in strength and energy from ordinary hydrogen bonds (O–H length 1.01 Å, O–D length 0.98 Å, D–O–D angle 106<sup>0</sup>). Commonly used molecular models use O–H lengths ~0.955 Å and 1.00 Å and H–O–H angles from ~105.5<sup>0</sup> to ~109.4<sup>0</sup>. The substitution of H with D atom affects the stability and geometry of hydrogen bonds in apparently rather complex way and may, through the changes in the hydrogen bond zero-point vibrational energies, alter the conformational dynamics of hydrogen (deuterium)-bonded structures of associates. In general, isotopic effects stabilize hydrogen bond with participation of deuterium, resulting in somewhat greater stability of associates formed from D<sub>2</sub>O molecules (Mosin & Ignatov, 2013b).

As a result of experiments on quasi-elastic neutron scattering the most important parameter was measured – the coefficient of self-diffusion of water at different temperatures and pressures. To analyse the self-diffusion coefficient on quasi-elastic neutron scattering, it is necessary to know the character of the moving of molecules. If they move in accordance with the “jump-wait“ model, then the “settled” life time (the time between jumps) of H<sub>2</sub>O molecule compiles 3.2 ps. The newest methods of femtosecond laser spectroscopy allow to estimate the lifetime of the broken hydrogen bonds: a proton needs 200 fs to find a partner.

The studying of the full details of the structure of associative elements in water can be made, considering all the parameters, by computer simulation or numerical experiment. For this in a given space a random ensemble of n H<sub>2</sub>O molecules is chosen which has the following physical parameters – the energy of

interatomic interactions, bond length, the arrangement of atoms and molecules, the most consistent with the diffraction data. Data thus obtained are then extrapolated to the actual water structure, and further used to calculate thermodynamic parameters. Data obtained by computer experiments, show that the nature of the thermal motion of the molecules in the liquids corresponds on the whole to a vibration of the individual H<sub>2</sub>O molecules near the equilibrium centers, with occasional jumps up to the new position.

Laboratory studies of antiviral activity of anolyte were performed at the National Reference Laboratory "Classical and African Swine Fever," section "Exotic and Especially Dangerous Infections" of the National Diagnostic and Research Veterinary Medical Institute, Sofia, Bulgaria. Experiments were conducted with anolyte obtained by the electrolysis apparatus "Wasserionisierer Hybrid PWI 2100" equipped with a 4 titanium electrodes coated with platinum. The disinfectant has a pH 3.2 and ORP 1070 mV. A 0.3% solution of chemically pure sodium chloride in distilled water was used to obtain it. The interaction of the anolyte with the virus suspension is carried out at a solution temperature of 22 °C. A cell culture of porcine origin that is sensitive to the CSF virus is used: a continuous cell line PK-15. Contamination of cell cultures is carried out with cell culture test virus 2.3 Bulgaria with titre 107,25 TCID<sub>50</sub>/ml and organ suspension of internal organs (spleen, kidney, lymph node) of wild boar originating from the last outbreak of CSF in Bulgaria in 2009. The titer of the established virus in the suspension is 10<sup>4,75</sup> TCID<sub>50</sub> ml. To establish virucidal activity, the prepared for contamination of cell culture inocula (cell culture virus) were treated with the following dilutions of anolyte in sterile distilled water 1:1 (50%), 1:2 (33.33%), 1:3 (25%), 1:4 (20%). These dilutions were mixed with inocula in proportion 1:1 (100 µl of virus suspension and 100 µl of the appropriate anolyte concentration). The time of action was conformed to the period, which is methodologically necessary to "capture" any virus present on the cell culture. Upon infection of a cell monolayer, the mixture was removed after the end of the exposure period of 1 h. Upon infection of a cell suspension, the mixture was not removed. To establish the virucidal activity of the anolyte on the CSF virus in organ suspension, a different formulation was used: the inoculum was mixed directly with concentrated anolyte in anolyte-inoculum ratios respectively 1:1; 3:1; 7:1 and 15:1. It is known that the growth of the virus does not cause a cytopathic effect, therefore, for demonstration of its presence, immunoperoxidase plates dyeing is used. The cells were fixed and the viral antigen was detected after binding to a specific antibody labeled with peroxidase. The organs exude 1 cm<sup>3</sup> of tissue, which is homogenized in a mortar with 9 ml of cell cultures medium containing antibiotics, in order to obtain a 10% organ suspension. Sterile sand is added to improve the homogenization. Preparations were left at room temperature for 1 h. They were centrifuged for 15 min at 2500 g. The supernatant was used to infect the cells. In case of cytotoxic effect, parallel dilutions of the homogenates were prepared in proportions 1:10 and 1:100. From the suspensions into multiwell (24-well) plates were added 200 µl of inoculum to cells with coverage of 50-80%. Cell cultures were incubated at 37 °C for 1 h in order to "capture" an eventual virus if present, they were rinsed once with PBS and fresh media was added. Alternatively, the plate was filled directly (in cell suspension), since the preliminary studies have found that anolyte did not induce a cytotoxic effect. Cell cultures were incubated for 72-96 h at 37 °C in a CO<sub>2</sub> incubator. The procedure with the positive and negative control samples was similar. The positive control sample was a reference strain of the virus of CSF. The immunoperoxidase technique was used. The fixation of the plates was carried out thermally for 3 h at 80 °C in a desiccator. In the processing was used a primary monoclonal antibody C 16 diluted 1:50, and secondary antibody RAMPO diluted 1:50. For immunoperoxidase staining was used 3% H<sub>2</sub>O<sub>2</sub> and AEC

(Dimethylformamide and 3 - Amino - 9 - ethylcarbazole) in acetate buffer. The antibody-antigen complex was visualized by the reaction of the peroxidase with the substrate.

A polymerase chain reaction in real time was carried out. Cell culture and organ suspensions were examined for the presence of CSF viral genome by polymerase chain reaction in real time (real-time RT-PCR, one step, TagMan), one-step according to Protocol of the Reference Laboratory for CSF of EU. For RNA extraction was used the test QIAamp Viral RNA Mini Kit, Qiagen, Hilden, Germany. The initial volume of the material was 140 µl, and the volume of elution – 60 µl. For amplification was used the test Qiagen OneStep RT-PCR Kit in a total volume of 25 µl, and template volume of 5 µl. In the reaction were included primers A 11 and A14, and probe TaqMan Probe - FAM - Tamra. Research was carried out with a thermocycler machine Applied Biosystems 7300 Real Time PCR System with temperature control for reverse transcription 50 °C – 30:00 min, inactivation of reverse transcriptase and activation of Taq 95 °C - 15:00 min, denaturation 95 °C - 00:10 min, extension 60 °C - 00:30 min at 40 cycles.

### 3. Results and discussions

Table 1 summarizes the results of studies carried out in the National Reference Laboratory to establish the virucidal effect of anolyte on cell culture (CC) suspension of the virus of CSF upon infection of the cell monolayer PK-15. Upon treatment of the viral inoculum with anolyte in a 1:1 dilution, there is no virus growth in the 4 infected wells of the plate, upon 1:2 dilution there is no growth in 2 of the wells, the other 2 we reported as positive. Upon treatment with anolyte at dilutions 1:3 and 1:4, the result is identical: no growth in one of the contaminated wells of the plate, and poor growth – in the other three.

Contamination of CC with:	Dilutions of anolyte (100 µl)	Total volume of the inoculum (µl)	Concentration of anolyte in %	Number of wells:	Result: positive/negative:
Virus 200 µl	-	200		4	4/0
Virus 100 µl	1:1	200	25	4	0/4
Virus 100 µl	1:2	200	16,51	4	2/2
Virus 100 µl	1:3	200	12,5	4	3/1
Virus 100 µl	1:4	200	10	4	3/1

Table 1. Virucidal action of anolyte on the cell culture suspension of the CSF virus upon infecting cell monolayer PK-15

Table 2 reflects the results of research conducted in National Reference Laboratory to establish the virucidal effect of anolyte on cell culture suspension of the CSF virus upon infecting cell suspension PK-15. Upon treatment of the viral inoculum with anolyte in a 1:1 dilution, virus growth is absent in the 4 infected wells of the plate, at a 1:2 dilution 2 of the wells lack growth, the other 2 wells were scored positive. Upon treatment with anolyte at dilutions 1:3 and 1:4 the result is identical: no growth in one of the contaminated wells of the plate, and poor growth – in the other three. The results obtained by infection of a cell monolayer and cell suspension are identical.



Contamination of CC with:	Dilutions of anolyte (100 µl)	Total volume of the inoculum (µl)	Concentration of anolyte in %	Number of wells:	Result: positive/negative:
Virus 200 µl	-	200		4	4/0
Virus 100 µl	1:1	200	25	4	0/4
Virus 100 µl	1:2	200	16,51	4	2/2
Virus 100 µl	1:3	200	12,5	4	3/1
Virus 100 µl	1:4	200	10	4	3/1

Table 2. Virucidal action of anolyte on the cell culture suspension of the CSF virus upon infecting cell suspension PK-15.

Table 3 summarizes the results of studies carried out in National Reference Laboratory to establish the virucidal effect of anolyte on organ suspension containing CSF virus upon infecting a cell monolayer PK-15. Upon treatment of the viral inoculum (organ suspension) with anolyte in all dilutions, there is no viral growth in the 4 infected wells of the plate.

Contamination of CC with:	Dilutions of anolyte (100 µl)	Total volume of the inoculum (µl)	Concentration of anolyte in %	Number of wells:	Result: positive/negative:
Virus 200 µl	-	200		4	4/0
Virus 100 µl	1:1	200	50	4	0/4
Virus 50 µl	3:1	200	75	4	0/4
Virus 25 µl	7:1	200	87	4	0/4
Virus 12,5 µl	15:1	200	94	4	0/4

Table 3. Virucidal action of anolyte on organ suspension containing CSF virus upon infecting cell monolayer PK-15.

In all likelihood anolyte has a destructive influence on the envelope of the CSF virus, where the main antigens (proteins) are. Studies of the viral inocula used in the tests by means of polymerase chain reaction in real time demonstrate the presence of a genome (a nucleic acid) in them, also after treatment with anolyte. Some shortening of the time is proved / decreased number of amplification cycles/, required for the formation of a fluorescent signal, respectively, a positive reaction for genome, closely correlated with the exposure in the treatment of the viral inocula. The longer the exposure of processing with anolyte, the sooner the presence of an RNA virus in the reaction is shown. According to three of the co-authors Atanasov, Ivanova and Karadjov, this is an indirect indication that anolyte destroys the virus envelope, which, in turn, facilitates the extraction of nucleic acid and its more rapid reading by the fluorescent signal. There is still no sufficient convincing evidence on the impact of different concentrations of anolyte on viral particles. Experiments carried out by Russian and German researchers are mainly with concentrated anolyte. The full virucidal effect obtained from them confirms our opinion for a strong virucidal action of electrochemically activated aqueous solution of sodium chloride. The differences in results obtained by us are due to the use of lower concentrations of active substances in our experiments. We attribute essential significance to the fact that we were given to determine the concentration limit (25%) of a well

demonstrated virucidal activity. Further studies to reduce the time of action, and the conducting of experiments in the presence of biofilm that protects viruses would be interesting.

Laboratory tests were performed at the National Reference Laboratory "Classical and African Swine Fever," section "Exotic and Especially Dangerous Infections" of the National Diagnostic and Research Veterinary Medical Institute, Sofia, Bulgaria. Experiments were conducted with anolyte obtained by the electrolysis apparatus "Wasserionisierer Hybrid PWI 2100", equipped with 4 platinum-coated titanium electrodes. In infected cells (positive reaction) the cytoplasm of the cells was stained in dark reddish brown color. Uninfected cells were colorless. (Fig. 2).

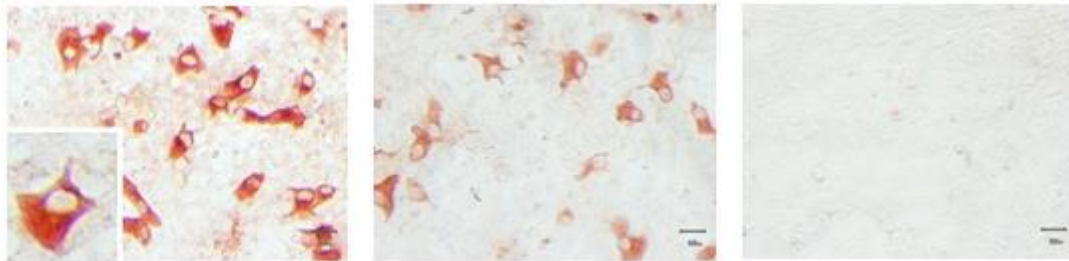


Figure. 2. Established presence of viral antigen (left) and a negative control (right).

#### 4. Nature of Hydrogen Bond in Liquids

The peculiarities of chemical structure of  $H_2O$  molecule and weak bonds caused by electrostatic forces and donor-acceptor interaction between hydrogen and oxygen atoms in  $H_2O$  molecules create favorable conditions for formation of directed intermolecular hydrogen bonds ( $O-H\dots O$ ) with neighboring  $H_2O$  molecules, binding them into complex intermolecular associates which composition represented by general formula  $(H_2O)_n$ , where  $n$  can vary from 3 to 50 (Keutsch & Saykally, 2011). The hydrogen bond - a form of association between the electronegative O oxygen atom and a H hydrogen atom, covalently bound to another electronegative O oxygen atom, is of vital importance in the chemistry of intermolecular interactions, based on weak electrostatic forces and donor-acceptor interactions with charge-transfer (Pauling, 1960). It results from interaction between electron-deficient H-atom of one  $H_2O$  molecule (hydrogen donor) and unshared electron pair of an electronegative O-atom (hydrogen acceptor) on the neighboring  $H_2O$  molecule; the structure of hydrogen bonding, therefore may be defined as  $O^{\ominus}H^{\oplus}-O$ . As a result, the electron of the H-atom due to its relatively weak bond with the proton easily shifts to the electronegative O-atom. The O-atom with increased electronegativity becomes partly negatively charged  $-\delta^-$ , while the H-atom on the opposite side of the molecule becomes positively charged  $-\delta^+$  that leads to the polarization of  $O^{\ominus}-H^{\oplus}$  covalent bond. In this process the proton becomes almost bared, and due to the electrostatic attraction forces are provided good conditions for convergence of  $O\dots O$  or  $O\dots H$  atoms, leading to the chemical exchange of a proton in the reaction  $O-H\dots O \leftrightarrow O\dots H-O$ . Although this interaction is essentially compensated by mutual repulsion of the molecules' nuclei and electrons, the effect of the electrostatic forces and donor-acceptor interactions for  $H_2O$  molecule compiles 5–10 kcal per 1 mole of substance. It is explained by negligible small atomic radius of hydrogen and shortage of inner electron shells,

which enables the neighboring H<sub>2</sub>O molecule to approach the hydrogen atom of another molecule at very close distance without experiencing any strong electrostatic repulsion.

The H<sub>2</sub>O molecule has four sites of hydrogen bonding – two uncompensated positive charges at hydrogen atoms and two negative charges at the oxygen atom. Their mutual disposition is characterized by direction from the centre of regular tetrahedron (nucleus of oxygen atom) towards its vertexes. This allows to one H<sub>2</sub>O molecule in condensed state to form up to 4 classical hydrogen bonds, two of which are donor bonds and the other two – acceptor ones (taking into consideration bifurcate (“two-forked”) hydrogen bond – 5) (Pasichnyk *et al.*, 2008).

A hydrogen bond according to Bernal–Fowler rules (Bernal & Fowler, 1933) is characterized by the following parameters:

a) an oxygen atom of each H<sub>2</sub>O molecule is bound with four neighboring hydrogen atoms: by covalent bonding with two own hydrogen atoms, and by hydrogen bonding – with two neighboring hydrogen atoms (as in the crystalline structure of ice); each hydrogen atom in its turn is bound with oxygen atom of neighbour H<sub>2</sub>O molecule.

b) on the line of oxygen atom – there can be disposed only one proton H<sup>+</sup>;

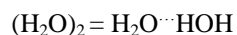
c) the proton, which takes part in hydrogen bonding situated between two oxygen atoms, therefore has two equilibrium positions: it can be located near its oxygen atom at approximate distance of 1 Å, and near the neighboring oxygen atom at the distance of 1.7 Å as well, hence both a usual dimer HO–H...OH<sub>2</sub> and an ion pair HO...H–OH<sub>2</sub> may be formed during hydrogen bonding, i.e. the hydrogen bond is part electrostatic (~90%) and part (~10%) covalent (Isaacs *et al.*, 2000). The state of “a proton near the neighboring oxygen” is typical for the interphase boundary, i.e. near water-solid body or water–gas surfaces.

d) the hydrogen bonding of a triad O–H...O possesses direction of the shorter O–H (→) covalent bond; the donor hydrogen bond tends to point directly at the acceptor electron pair (this direction means that the hydrogen atom being donated to the oxygen atom acceptor on another H<sub>2</sub>O molecule).

The most remarkable peculiarity of a hydrogen bond consists in its relatively low strength; it is 5–10 times weaker than a chemical covalent bond (Pimentel & McClellan, 1960). In respect of energy, hydrogen bond has an intermediate position between covalent bonds and intermolecular van der Waals forces, based on dipole-dipole interactions, holding the neutral molecules together in gasses or liquefied or solidified gasses. Hydrogen bonding produces interatomic distances shorter than the sum of van der Waals radii, and usually involves a limited number of interaction partners. These characteristics become more substantial when acceptors bind H-atoms from more electronegative donors. Hydrogen bonds hold H<sub>2</sub>O molecules on 15% closer than if water was a simple liquid with van der Waals interactions. The hydrogen bond energy compiles 5–10 kcal/mole, while the energy of O–H covalent bonds in H<sub>2</sub>O molecule – 109 kcal/mole (Arunan *et al.*, 2011). The values of the average energy ( $\Delta E_{H...O}$ ) of hydrogen H...O-bonds between H<sub>2</sub>O molecules make up  $0.1067 \pm 0.0011$  eV (Antonov & Galabova, 1992). With fluctuations of water temperature the average energy of hydrogen H...O-bonds in of water molecule associates changes. That is why hydrogen bonds in liquid state are relatively weak and unstable: it is thought that they can easily form and disappear as the result of temperature fluctuations (Ignatov & Mosin, 2013a).

Another key feature of hydrogen bond consists in its cooperativity coupling. Hydrogen bonding leads to the formation of the next hydrogen bond and redistribution of electrons, which in its turn promotes the formation of the following hydrogen bond, whose length increases with distance. Cooperative hydrogen

bonding increases the O–H bond length, at the same time causing a reduction in the H...O and O...O distances (Goryainov, 2012). The protons held by individual H<sub>2</sub>O molecules may switch partners in an ordered manner within hydrogen networks (Bartha *et al.*, 2003). As a result, aqueous solutions may undergo autoprotolysis, i.e. the H<sup>+</sup> proton is released from H<sub>2</sub>O molecule and then transferred and accepted by the neighboring H<sub>2</sub>O molecule resulting in formation of hydronium ions as H<sub>3</sub>O<sup>+</sup>, H<sub>5</sub>O<sub>2</sub><sup>+</sup>, H<sub>7</sub>O<sub>3</sub><sup>+</sup>, H<sub>9</sub>O<sub>4</sub><sup>+</sup>, etc. This leads to the fact, that water should be considered as associated liquid composed from a set of individual H<sub>2</sub>O molecules, linked together by hydrogen bonds and weak intermolecular van der Waals forces (Liu *et al.*, 1996). The simplest example of such associate can be a dimer of water:



The energy of the hydrogen bonding in the water dimer is 0.2 eV (~5 kcal/mol), which is larger than the energy of thermal motion of the molecules at the temperature of 300 K. Hydrogen bonds are easily disintegrated and re-formed through an interval of time, which makes water structure quite unstable and changeable (George, 1997). This process leads to structural inhomogeneity of water characterizing it as an associated heterogeneous two-phase liquid with short-range ordering, i.e. with regularity in mutual positioning of atoms and molecules, which reoccurs only at distances comparable to distances between initial atoms, i.e. the first H<sub>2</sub>O layer. As it is known, a liquid in contrast to a solid body, is a dynamic system: its atoms, ions or molecules, keeping short-range order in mutual disposition, participate in thermal motion, the character of which is much more complicated than that of crystals. For example H<sub>2</sub>O molecules in liquid state under normal conditions (1 atm, 22 °C) are quite mobile and can oscillate around their rotation axes, as well as perform the random and directed shifts. This enabled some individual molecules due to cooperative interactions to “jump up” from one place to another in an elementary volume of water. Random motion of molecules in liquids causes continuous changes in the distances between them. The statistical character of ordered arrangement of molecules in liquids results in fluctuations – continuously occurring deviations not only from average density, but from average orientation as well, because molecules in liquids are capable to form groups, in which a particular orientation prevails. Thus, the smaller these deviations are, the more frequently they occur in liquids.

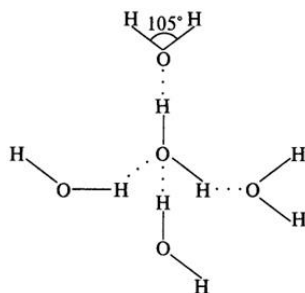


Figure 3. Hydrogen bonding between four individual H<sub>2</sub>O molecules. The value of the angle between the covalent H–O–H bond in H<sub>2</sub>O molecule is shown.

The further important feature is that the hydrogen bonds are spatially oriented. As each H<sub>2</sub>O molecule has four sites of hydrogen bond formation (two non-shared electron pairs at an oxygen atom and two

uncompensated positive charges at a hydrogen atom), one H<sub>2</sub>O molecule in a condensed state is capable to form hydrogen bonds with four H<sub>2</sub>O molecules (two donor and two acceptor) (Figure 3), which results in forming a tetrahedron crystal structure clearly observed in ice crystals.

## 5. Structural Models of Water

There are several groups of models, describing structure of liquids – microcrystalline, quasicrystalline, continuous, fractal and fractal-clathrate models. The microcrystalline model of J. Bernal and P. Fowler suggests that water is a nonequilibrium 2-phase liquid containing groups of oriented molecules – microcrystals with several dozens or hundreds of molecules (Bernal & Fowler, 1933; Timothy & Zwier, 2004). Within each microcrystal in liquid a solid body ordering (long-range order) is strictly kept. As water is denser than ice, it is assumed that its molecules are allocated in a different way than in ice: like the atoms of silicon in mineral tridymite or in its more solid modification of quartz. The intermittent increase in water density from 0 to 3.98 °C and other anomalous properties of water was explained by the existence of tridymite component at low temperatures (Pople, 1951).

Quasicrystalline model by analogy with a quasicrystal, i.g. a structure that is ordered but not periodic (Nemukhin, 1996), suggests that relative disposition of particles in liquids is nearly the same as in crystals; deviation from regularity increases with the distance from the initial H<sub>2</sub>O molecule; far apart at longer distances there is no regularity in the disposition of H<sub>2</sub>O molecules. Each H<sub>2</sub>O molecule is surrounded by the four neighbouring ones, which are arranged around it in quite the same way, as they are in an ice crystal. However, in the second layer there appear deviations from regularity rapidly increasing with distance from the initial H<sub>2</sub>O molecule. Studies of X-ray scattering in liquids consisting of polyatomic molecules, revealed not only some regular arrangement of H<sub>2</sub>O molecules, but consistent pattern in mutual orientation of the molecules (Petkov *et al.*, 2012). This orientation becomes even more expressed for the polar molecules because of the hydrogen bonding effect.

Kinetic theory of liquids proposed by Y.I. Frenkel, also called a “jump-wait“ model, explains the structural properties of liquids by peculiarities of thermal motion of their molecules (Frenkel, 1975). The thermal motion of H<sub>2</sub>O molecules is characterized by two parameters: a period of oscillation of H<sub>2</sub>O molecule around an equilibrium position and a period of “settled life”, i.e. period of oscillation around one particular equilibrium position. Average time of “settled life” of a H<sub>2</sub>O molecule, within which H<sub>2</sub>O molecules keep unchanged equilibrium orientation is called relaxation time  $\tau$ :

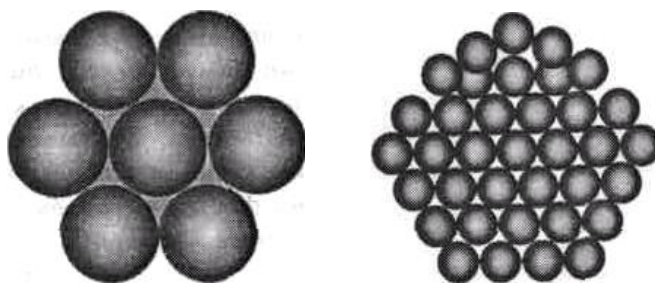
$$\tau = \tau_0 \times e^{W/RT},$$

where  $\tau_0$  is an average period of oscillations of a H<sub>2</sub>O molecule around an equilibrium position (sec), W – a value of potential energy barrier, separating two neighboring equilibrium positions from each other (J), R – Boltzmann constant (J/K), T – absolute temperature (K).

According to calculations, the relaxation time at room temperature makes up  $\sim 4.5 \cdot 10^{-12}$  sec, while the period of one oscillation of H<sub>2</sub>O molecules –  $10^{-12}$ – $10^{-13}$  sec. That is why each H<sub>2</sub>O molecule performs approximately 100 oscillations relative to the same equilibrium position before changing its place. Due to thermal fluctuations one H<sub>2</sub>O molecule within its “settled life” period of time oscillates around an equilibrium position, after then jumps up to new location and it continues to fluctuate up to the next jump. Through these abrupt movements of molecules in liquids occurs diffusion, which, in contrast to the

continuous diffusion in gases, is called diffusion jump. With increase in temperature the period of “settled life” of  $H_2O$  molecules in a temporary state of equilibrium is changed in structures of water closest to a gas, in which translational and rotational motions of  $H_2O$  molecules prevail. Theoretical studies show that, in liquids, along with the fluctuation, each neighboring molecule is being restructured. Being in oscillating state, the molecules in the liquid are displaced each time by a certain distance (less than the interatomic distance), causing continuous diffusion. It is believed that in the liquefied inert gases and metals dominates continuous diffusion, while for associated liquids as water is more likely the jump diffusion mechanism. The thermal motion of  $H_2O$  molecules leads to continuous changes in distances between them, which cause fluctuations – continual deviations not only from the average density, but from the average orientation of the molecules as well, because  $H_2O$  molecules can form groups in which a certain orientation predominates. An attempt to change the water volume (even by small quantity) triggers the process of deformation of hydrogen bonds, that fact may explain low water compressibility. Ice melting also causes weakening and deformation of hydrogen bonds, which makes water denser than ice. At the temperature  $3.98\text{ }^\circ\text{C}$  water acquires anomalous state, in which the quasicrystalline phase is maximally densified by filling up of ice carcass hollows with  $H_2O$  molecules. Further increase in temperature and energy of thermal motion of  $H_2O$  molecules leads to the gradual disintegration of associated water structures and to the partial rupture of hydrogen bonds with essential reduce of the “settled life” of each  $H_2O$  molecule in water associates.

The continuous and “fractal” models consider water as a complex dynamic system with a hydrogen network, forming the empty cavities and non-bonded  $H_2O$  molecules distributed within the network. The structure is based upon dimensional carcasses of individual  $H_2O$  molecules, joined together into a multi-molecular associate similar to a clathrate having a configuration of a regular polyhedron (Samoilov, 1963). Stated geometrically, this model represents the packed spheres with varying degrees of packaging. Thus, the pentagonal packing of spheres, showed in Figure 4b, is denser, than the sphere packing model in Figure 4a (its density is 72%). Analogous structure has clathrate hydrates (gas clathrates) – crystalline water-based solids physically resembling ice, in which small non polar gas molecules are placed inside cavities of hydrogen bonded  $H_2O$  molecules.



a)

b)

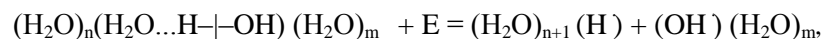
Figure 4. The sphere (a) and the pentagonal (b) packing of balls representing  $H_2O$  molecules in clusters.

In 1957 S.Frank and W. Wen proposed a model, postulating arbitrary formation of cyclic associates in water, which presumably had random groups of water associates – the “flickering clusters” with general formula

$(\text{H}_2\text{O})_n$ , which are in a dynamic equilibrium with free  $\text{H}_2\text{O}$  molecules (Henry et al., 1957). The hydrogen bonds between  $\text{H}_2\text{O}$  molecules are in dynamic equilibrium; they are constantly broken and re-formed in new configurations within a certain time interval; these processes are occurred cooperatively within short-living associated groups of  $\text{H}_2\text{O}$  molecules (clusters), which life spans are estimated from  $10^{-10}$  to  $10^{-11}$  sec.

Water associates evidently may have polymer structure, because hydrogen bond is on 10% partially covalent bond (Isaacs *et al.*, 2000). In 1990 G.A. Domrachev and D.A. Selivanovsky formulated a model of  $\text{H}_2\text{O}$ -polymers based on the existence of mechanochemical reactions of ionization and dissociation of water in aqueous solutions (Domrachev & Selivanovsky, 1990). Water was thought as dynamically unstable quazi-polymer, composed of  $(\text{H}_2\text{O})_n$  blocks with partially covalent by 10% hydrogen bonds, permitting at least to 10% of  $\text{H}_2\text{O}$  molecules to combine in sufficiently long-lived polymer associates. Similarly with mechanochemical reactions in polymers, in case of mechanical impact on water, the energy absorbed by water required for splitting up the H–OH bond, concentrates in a micro-scale area of the liquid water structure.

The splitting up reaction of the H–OH bond in water polymer associates is expressed by the following equation:



where E – the energy of the H–OH bond, 460 κJ/mole; the dot denotes an unpaired electron.

Splitting up of the H–OH bond is accompanied by formation of new disordered bonds between “fragments” of the initial molecules, leading to the formation of fluctuation areas with different density fluctuations that can be observed in aqueous solutions.

Another interesting physical phenomenon was discovered by A. Antonov in 2005 (Antonov, 2005). It was established experimentally that at evaporation of water droplet, the contact angle  $\theta$  decreases discretely to zero, whereas the diameter of the droplet changes insignificantly. By measuring this angle within a regular time intervals a functional dependence  $f(\theta)$  can be determined, which is designated by the spectrum of the water state. For practical purposes by registering the spectrum of water state it is possible to obtain information about the averaged energy of hydrogen bonds in an aqueous sample. For this purpose the model of W. Luck is used, which considers water as an associated liquid, consisting of O–H...O–H groups (Luck *et al.*, 1980). The major part of these groups is designated by the energy of hydrogen bonds ( $-E$ ), while the others are free ( $E = 0$ ). The energy distribution function  $f(E)$  is measured in electron-volts ( $\text{eV}^{-1}$ ) and may be varied under the influence of various external factors on water as temperature and pressure.

For calculation of the function  $f(E)$ , experimental dependence between the water surface tension ( $\theta$ ) and the energy of hydrogen bonds ( $E$ ) is established:

$$f(E) = b \times f(\theta) / 1 - (1 + b \times E)^2)^{1/2},$$

where  $b = 14.33 \text{ eV}^{-1}$

The energy of hydrogen bonds ( $E$ ) is measured in electron-volts ( $\text{eV}$ ) and is designated by the spectrum of

energy distribution. The water spectrum is characterized by a non-equilibrium process of water droplets evaporation, thus the term “non-equilibrium energy spectrum of water” (NES) is applied.

The difference  $\Delta f(E) = f(\text{samples of water}) - f(\text{control sample of water})$  is called the “differential non-equilibrium energy spectrum of water” (DNES).

DNES is a measure of changes in the structure of water as a result of external influences. The cumulative effect of all other factors is the same for the control sample of water and the water sample, which is under the influence of this impact.

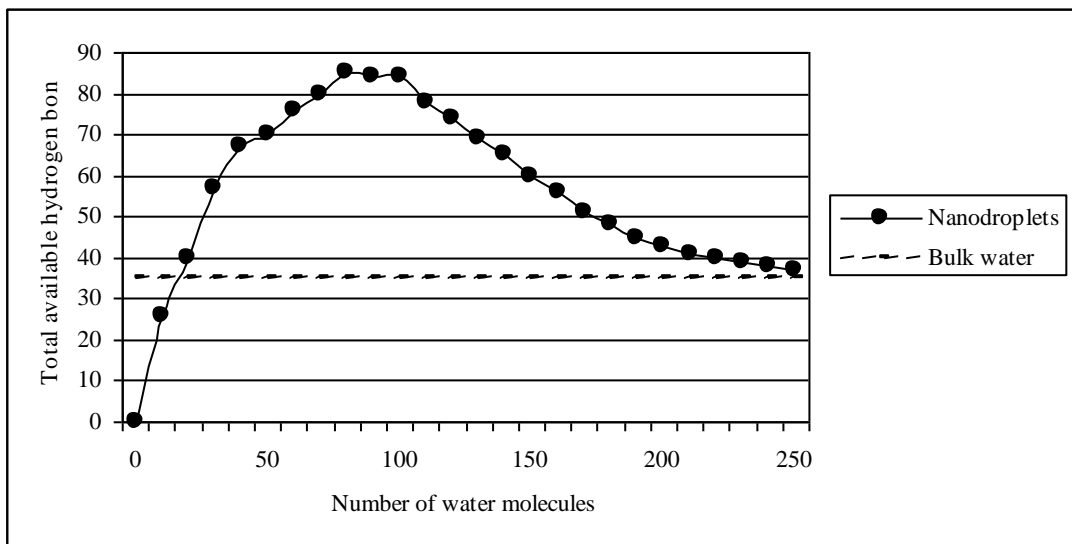


Figure 5. The total number of hydrogen bonds depending on the number of water molecules in clusters.

In 2005 R. Saykally (University of California, USA) calculated the possible number of hydrogen bonds and the stability of water clusters depending on the number of H<sub>2</sub>O molecules (Figure 6) (Saykally, 2005). The possible number of hydrogen bonds (100) depending on the number of H<sub>2</sub>O molecules (250) in clusters was also estimated (Sykes, 2007). O. Loboda and O.V. Goncharuk provided data about the existence of icosahedral water clusters consisting of 280 H<sub>2</sub>O molecules with average size up to 3 nm (Loboda & Goncharuk, 2010). The ordering of water molecules into associates corresponds to a decrease in the entropy (randomness), or decrease in the overall Gibbs energy ( $G = \Delta H - T\Delta S$ ). This means that the change in enthalpy  $\Delta H$  minus the change in entropy  $\Delta S$  (multiplied by the absolute temperature  $T$ ) is a negative value. These results are consistent with our data on research of NES spectrum of water on which we can base our conclusion about the number of H<sub>2</sub>O molecules in water clusters. NES spectrum of water has energy ranges from -0.08 to -0.14 eV (Figure 7). The spectral range lies in the middle infrared range from 8 to 14  $\mu\text{m}$  ("window" of the atmosphere transparency to electromagnetic radiation). Under these conditions, the relative stability of water clusters depends on external factors, primarily on the temperature.



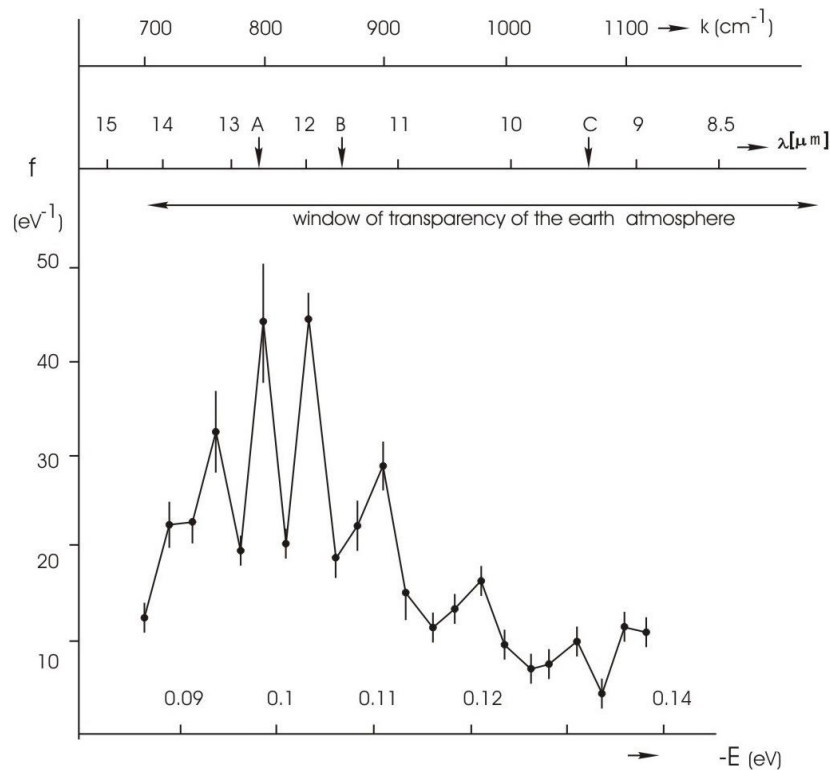


Figure 6. NES-spectrum of deionized water (chemical purity 99.99%, pH = 6.5–7.5, total mineralization 200 mg/l, electric conductivity 10  $\mu\text{S}/\text{cm}$ ). The horizontal axis shows the energy of the H...O hydrogen bonds in the associates  $-E$  (eV). The vertical axis – energy distribution function  $-f$  ( $\text{eV}^{-1}$ ).  $k$  – the vibration frequency of the H–O–H atoms ( $\text{cm}^{-1}$ );  $\lambda$  – wavelength (mm).

It was shown that the  $\text{H}_2\text{O}$  molecules change their position in clusters depending on the energy of intermolecular H...O hydrogen bonds. The values of the average energy ( $E_{\text{H}\dots\text{O}}$ ) of hydrogen bonds between the  $\text{H}_2\text{O}$  molecules in the formation of cluster associates with formula  $(\text{H}_2\text{O})_n$  have an average energy of the samples with deionized water  $0.1067 \pm 0.0011$  eV (1150 measurements). As the energy of hydrogen bonds between  $\text{H}_2\text{O}$  molecules increases up to  $-0.14$  eV, the cluster formation of water becomes “destructuring”. In this case, the energy redistribution between the individual  $\text{H}_2\text{O}$  molecules occurs (Figure 6).

All these data indicate that water is a complex associated non-equilibrium liquid consisting of associative groups containing, according to the present data, from 3 to 20 individual  $\text{H}_2\text{O}$  molecules (Tokmachev *et al.*, 2010). Associates can be perceived as unstable groups (dimers, trimers, tetramers, pentamers, hexamers etc.) in which  $\text{H}_2\text{O}$  molecules are linked by van der Waals forces, dipole-dipole and other charge-transfer interactions, including hydrogen bonding. At room temperature, the degree of association of  $\text{H}_2\text{O}$  molecules may vary from 2 to 6. In 1993 K. Jordan (USA) (Tsai & Jordan, 1993) calculated the possible structural modifications of small water clusters consisting of six  $\text{H}_2\text{O}$  molecules (Figure 7a–c). Subsequently, it was shown that  $\text{H}_2\text{O}$  molecules are capable of hydrogen bonding by forming the structures representing topological 1D rings and 2D chains composed from numerous  $\text{H}_2\text{O}$  molecules. Interpreting the

experimental data, they are considered as pretty stable elements of the structure. According to computer simulations, clusters are able to interact with each other through the exposed protons on the outer surfaces of hydrogen bonds to form new clusters of more complex composition.

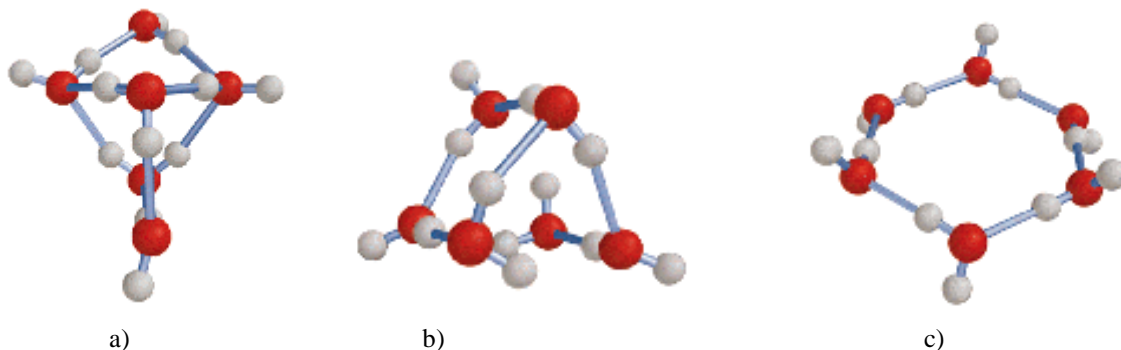


Figure 7. Calculation of small water cluster structures (a–c) with general formula  $(\text{H}_2\text{O})_n$ , where  $n = 6$  (Tsai & Jordan, 1993).

In 2000 the structure of the trimer water was deciphered, and in 2003 – tetramer, pentamer and the water hexamer (Wang & Jordan, 2003). Structures of water clusters with formula  $(\text{H}_2\text{O})_n$ , where  $n = 3-5$ , similar to the cage structure. Hexagonal structure with  $n = 6$ , consisting of six  $\text{H}_2\text{O}$  molecules at the hexagon vertices, is less stable than the cage structure. In the hexagon structure four  $\text{H}_2\text{O}$  molecules can be cross-linked by hydrogen bonds (Figure 8).

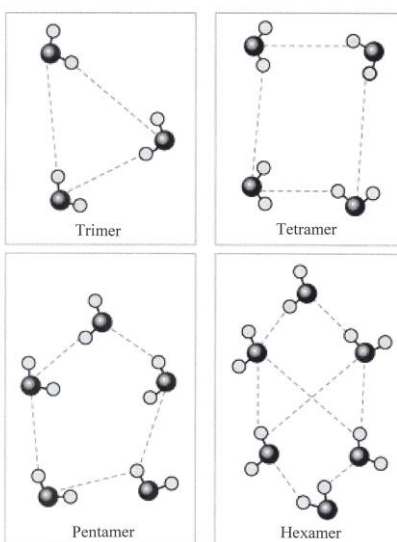


Figure 8. Cluster structure of a trimer, tetramer, pentamer and hexamer of water.

Quantum-chemical calculations of middle size clusters with the general formula  $(\text{H}_2\text{O})_n$ , where  $n = 6-20$ , have shown that the most stable structures are formed by the interaction of tetrameric and pentameric structures (Maheshwary *et al.*, 2001; Choi & Jordan, 2010). Thus the structures of  $(\text{H}_2\text{O})_n$ , where  $n = 8, 12$ ,

16, and 20 are cubic, and structures  $(\text{H}_2\text{O})_n$  where  $n = 10$  and  $15$  – pentagons. Other structures with  $n = 9$ ,  $11$ ,  $13$ ,  $14$ ,  $17$ ,  $18$  and  $19$  evidently have a mixed composition. Large tetrahedron clusters as  $(\text{H}_2\text{O})_{196}$ ,  $(\text{H}_2\text{O})_{224}$ ,  $(\text{H}_2\text{O})_{252}$  (Figure 10) composed from the smaller ones formed a vertex of a  $(\text{H}_2\text{O})_{14}$  tetrahedron are also described (Chaplin, 2011).

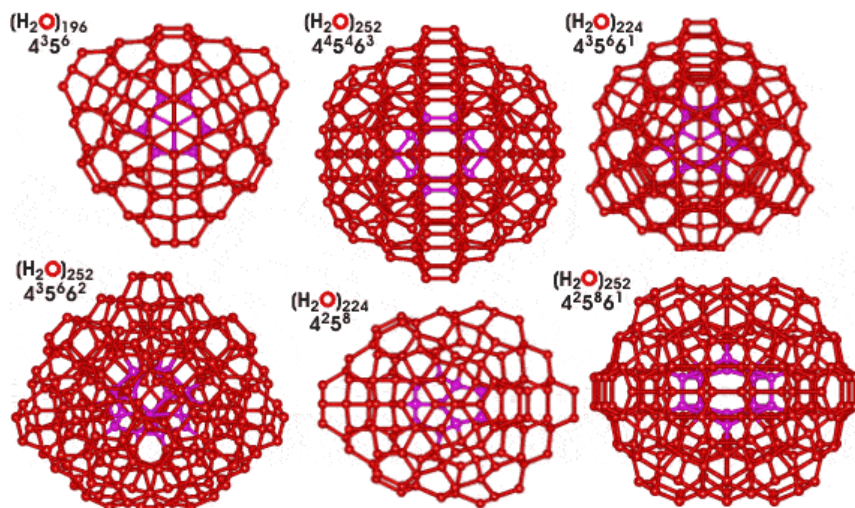


Figure 10. Tetrahedron water clusters  $(\text{H}_2\text{O})_n$  with different symmetry ( $n = 196, 224, 252$ ).

The clusters, evidently, may be rather stable under a certain conditions, and can be obtained in the isolated state within a very short interval of time. There is also a reason to believe that the charged ions stabilize the clusters. Therefore, the clusters can be divided into positively and negatively charged ionic clusters –  $[\text{H}^+(\text{H}_2\text{O})_n]^+$ ,  $[\text{OH}^-(\text{H}_2\text{O})_n]^-$ , and not having a charge – neutral clusters with general formula  $(\text{H}_2\text{O})_n$ . Clusters, containing 20 individual  $\text{H}_2\text{O}$  molecules and a proton in the form of hydronium ion  $\text{H}_3\text{O}^+$  (“magic” number) form the most stable ionic clusters  $[(\text{H}_2\text{O})_{20}\text{H}_3\text{O}]^+$  or  $[(\text{H}_2\text{O})_{21}\text{H}]^+$  (Figure 11) (Cui *et al.*, 2006). It is assumed that the stability of ionic clusters is due to the special clathrate structure in which 20  $\text{H}_2\text{O}$  molecules can form 12 pentagonal dodecahedron, which contain the  $\text{H}_3\text{O}^+$  ions. It occurs because of all the clusters only the dodecahedron has cavities large enough to accommodate a bulky  $\text{H}_3\text{O}^+$  ion. Subsequently, due to cooperative interactions  $\text{H}_3\text{O}^+$  is further able to move to the surface of the cluster and lose a proton  $\text{H}^+$  leading to the formation of hydronium ions like  $\text{H}_5\text{O}_2^+$ ,  $\text{H}_7\text{O}_3^+$ , and  $\text{H}_9\text{O}_4^+$ , fixed on the surface of the cluster. These data show the diversity of supposed water structures and the complexity of molecular interactions between the different water clusters, the nature of which we are only beginning to understand.

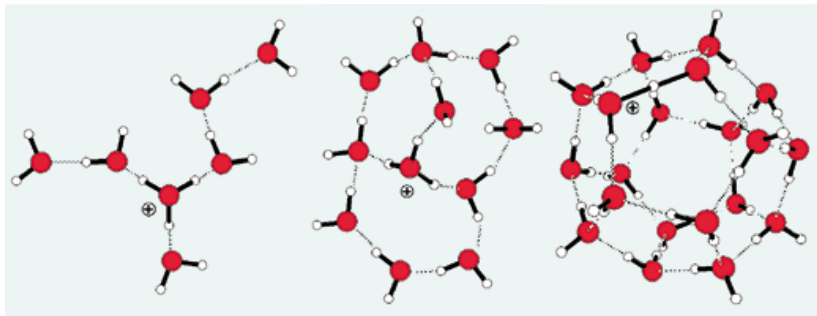


Figure 11. Formation of ionic clusters  $[(\text{H}_2\text{O})_{20}\text{H}_3\text{O}]^+$  or  $[(\text{H}_2\text{O})_{21}\text{H}]^+$  with captured hydronium ion  $\text{H}_3\text{O}^+$ .

It is reasonable that the structure of liquid water should be related to the structure of hexagonal ice, formed from  $\text{H}_2\text{O}$  tetrahedrons, which exist under atmospheric pressure. In the computer simulation  $\text{H}_2\text{O}$  tetrahedrons grouped together, to form a variety of 3D-spatial and 1D, 2D-planar structures, the most common of which is hexagonal structure where 6  $\text{H}_2\text{O}$  molecules (tetrahedrons) are combined into a ring. A similar type of structure is typical for ice  $\text{I}_h$  crystals. When ice melts, its hexagonal structure is destroyed, and a mixture of clusters consisting of tri-, tetra-, penta-, and hexamers of water and free  $\text{H}_2\text{O}$  molecules is formed. Structural studies of these clusters are significantly impeded, since the water is perceived as a mixture of different clusters that are in dynamic equilibrium with each other.

S. Zenin (Russia) calculated a cluster model based on a minimum "quantum" of water (Zenin, 1999), which is a 4 triangular tetrahedron composed of four 12 pentagonal dodecahedrons (Figure 12). The "quantum" consisted of 57  $\text{H}_2\text{O}$  molecules interacting with each other at the expense of free hydrogen bonds exposed on the surface. Of 57  $\text{H}_2\text{O}$  molecules in the "quantum" 17  $\text{H}_2\text{O}$  molecules compose tetrahedral completely hydrophobic, i.e. saturated with four hydrogen bonds in the central carcass, and four dodecahedra, on the surface of each there are 10 centers for the formation of hydrogen bond (O–H or O). 16 "quanta" form a bigger cluster structure consisted from 912  $\text{H}_2\text{O}$  molecules similar to a tetrahedron.

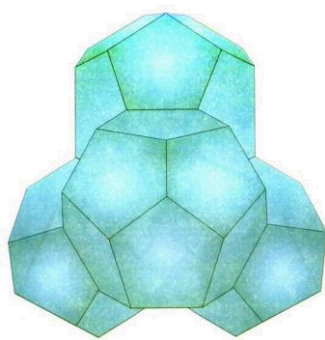


Figure 12. Model of water associate from 57  $\text{H}_2\text{O}$  molecules. Tetrahedron of four dodecahedrons ("quantum") according to the model of S. Zenin (Zenin, 1999).

M. Chaplin (London South Bank University, UK) (Chaplin, 2011) calculated the water structure based on 20 triangular icosahedron (Figure 13). The structure is based on minimal tetrahedral water cluster, consisting of 14  $\text{H}_2\text{O}$  molecules. Arrangement of 20 of these 14-molecule structures forms an icosahedral

network consisting from 280 H<sub>2</sub>O molecules. Each 280-molecule in icosahedral contains several substructures with each H<sub>2</sub>O molecule involved in four hydrogen bonds; two as donors and two as acceptors. 13 overlapping icosahedra may form a larger cluster (tricontahedron) consisting from 1820 H<sub>2</sub>O molecules, which have twice as much H<sub>2</sub>O molecules than in the previous model.

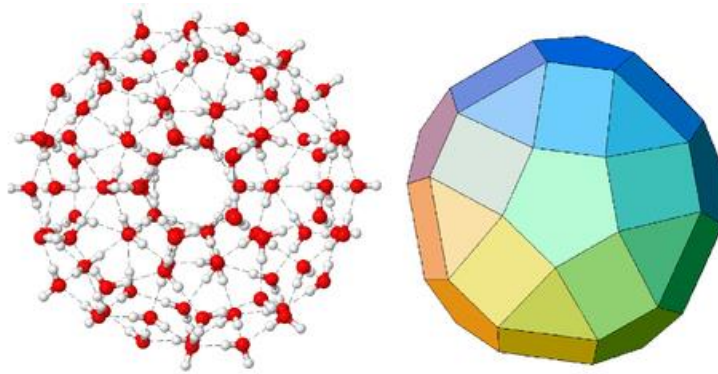


Figure 13. Icosahedron cluster based on 100 H<sub>2</sub>O molecules and the underlying structure.

The research with NES method of alkaline (catholyte) and acid (anolyte) solution with information for the possible number of hydrogen bonds as percent of water molecules with different values of distribution of energies (Table 4). These distributions are basically connected with restructuring of H<sub>2</sub>O molecules with the same energies.

<b>-E(eV)</b> x-axis	<b>Catholyte</b> y-axis (eV <sup>-1</sup> )	<b>Anolyte</b> y-axis (eV <sup>-1</sup> )	<b>-E(eV)</b> x-axis	<b>Catholyte</b> y-axis (eV <sup>-1</sup> )	<b>Anolyte</b> y-axis (eV <sup>-1</sup> )
0.0937	0	0	0.1187	0	16.7
0.0962	0	0	0.1212	16.7	0
0.0987	0	0	0.1237	0	0
0.1012	16.7	16.7	0.1262	0	0
0.1037	0	0	0.1287	0	0
0.1062	0	0	0.1312	8.4	24.8
0.1087	0	0	0.1337	8.4	8.4
0.1112	0	0	0.1362	0	0
0.1137	0	16.7	0.1387	49.8	16.7
0.1162	0	0	–	–	–

Table 4. Mathematical model of alkaline (catholyte) and acid (anolyte) solution in electrochemical

activation of sodium chloride as a percentage distribution by energies among water molecules (Ignatov, Mosin, 2014). The analysis is made by non-equilibrium energy spectrum (NES) (Antonov, 1990, Ignatov, 1998).

## 5. Conclusion

The experimental data obtained during the last years suggest that water is a complex dynamic associative system, consisting of tens and possibly hundreds of individual H<sub>2</sub>O molecules bonding by multiple intermolecular hydrogen bonds, being in a state of dynamic equilibrium. Up till now the existence of associative water clusters with general formula (H<sub>2</sub>O)<sub>n</sub>, where n = 3–20 has been scientifically proven. Although calculated structural models explain pretty well many anomalous properties of water and being in a good agreement with the experimental data on the diffraction of X-rays and neutrons, Raman, Compton scattering and EXAFS-spectroscopy, they are the most difficult to agree with the dynamic properties of water – flow, viscosity and short relaxation times, which are measured by picoseconds.

Research findings of antimicrobial action of acid solution (catholyte)

1. Anolyte did not affect the growth of the cell culture, PK-15.
2. Anolyte administered at a concentration of 25%, exhibits a strong virucidal effect on a cell culture virus and a weaker antiviral activity at concentrations of 16.51%, 12,5% and 10%.
3. Anolyte exerted a strong virucidal effect at a concentration of 50%, 75%, 87% and 94% over in CSF viruses in organ suspension.
4. At concentrations above 50% anolyte can be successfully used to achieve efficient disinfection of surfaces in virological laboratories.

## References

- Antonov, A. (2005) Research of the nonequilibrium processes in the area in allocated systems. *Diss. thesis doctor of physical sciences*. Sofia: Blagoevgrad: 1–255.
- Atanasov, A., Karadzhev, S., Ivanova, E., Mosin, O. V.&Ignatov, I. (2014) Study of the Effects of Electrochemical Aqueous Sodium Chloride Solution (Anolyte) on the Virus of Classical Swine Fever Virus. Mathematical Models of Anolyte and Catholyte as Types of Water, *Journal of Medicine, Physiology and Biophysics*, **4**: 1-26.
- Cascarini de Torre, L.E., Fertitta, A.E., Flores, E.S., Llanos, J.L. & Bottani, E.J. (2004) Characterization of shungite by physical adsorption of gases. *J. Argent. Chem. Soc.*, **92**(4–6): 51–58.
- Golubev, E.A. (2000) Local supramolecular structures shungite carbon, in Proceedings of the Int. Symp. "Carbon-formation in geological history", Petrozavodsk: Publishing House of the Karelian Research Center, Russian Academy of Sciences: 106–110 [in Russian].
- Gorshteyn, A.E., Baron, N.Y. & Syrkina, M.L. (1979) Adsorption properties of shungites. *Izv. Vysshykh Uchebn. Zaved. Khimia i Khim. Technol.*, **22**(6): 711–715 [in Russian].
- Depner, K., Bauer, T.&Liess, B. (1992) Thermal and pH stability of pestiviruses. *Rev. Sci. Tech.* **11**: 885-893.
- Edwards, 2000&Edwards, S. (2000): Survival and inactivation of classical swine fever virus. *Veterinary*

*Microbiology* **73**: 175-181.

European Commission (2002) Commission Decision of February 2002 approving a diagnostic manual establishing diagnostic procedures, sampling methods and criteria for evaluation of the laboratory tests for the confirmation of CSF, (2002/106/EC), *Chapter VII. Off.J.Eur.Union*, L39: 71-88.

European Commission (2003) Diagnostic techniques and vaccines for FMD, CSF, AI and some other important OIE List A diseases. Report. *Committee on Animal Health and Animal Welfare*, Brussels, 1-150.

Haas, B., Ahl, R., Bohm, R. & Strauch, D. (1995): „Inactivation of viruses in liquid manure“. *Rev. Sci. Tech.* **14**: 435-445.

Hanaoka, K. (2001): Antioxidant effects of reduced water produced by electrolysis of sodium chloride solutions, *Journal of Applied Electrochemistry*, **31**: 1307–1313

Khavari-Khorasani, G. & Murchison, D.G. (1979) The nature of carbonaceous matter in the Karelian shungite. *Chem. Geol.*, **26**: 165–82.

Moenning, V. (2000): Introduction to classical swine fever: virus, disease and control policy, *Vet. Microbiology*, **73**: 93-102.

Mortrivski, A., Nedelchev, N. & Karadzhov, S. (2009) Infectious Diseases on the Industrial Produced Swine in Bulgaria, *Veterinary Medicine Archive* **2**(2): 3-16. [in Czech].

Volkova, I.B. & Bogdanov, M.V. (1986) Petrology and genesis of the Karelian shungite-high rank coal. *Int. J. Coal Geol.*, **6**: 369–79.

Ignatov, I., Antonov, A. & Galabova, T. (1998) Medical Biophysics – Biophysical Fields of Man, *Gea Libris*, Sofia.

Ignatov, I., Antonov, A. & Galabova, T., (2002) Scientific Research Studies with Christos Drossinakis (October 2001 – October 2002), *Int. Conference “Man and Nature”*, SRCMB, Sofia.

Ignatov, I. (2005) Energy Biomedicine, *Gea-Libris*, Sofia: 1–88.

Ignatov, I. (2007) There are not Reliable Results with Research with Infrared Spectroscopy of Homeopathic Solutions after Avogadro’s Number, *Ministry of Health*, 196-199. [in Russian]

Marinov, M., Ignatov, I. (2008) Color Kirlian Spectral Analysis. Color Observation with Visual Analyzer, *Euromedica*, Hanover, 57-59

Ignatov, I. (2010) Which water is optimal for the origin (generation) of life? *Euromedica*, Hanover: 34-35.

Ignatov, I. (2011) Entropy and time in living matter, *Euromedica*: 74.

Ignatov, I., Tsvetkova, V. (2011) Water for the Origin of Life and “Informationability” of Water, Kirlian (Electric Images) of Different Types of Water, *Euromedica*, Hanover: 62-65.

Ignatov, I. (2012) Origin of Life and Living Matter in Hot Mineral Water, Conference on the Physics, Chemistry and Biology of Water, *Vermont Photonics*, USA.

Ignatov, I., & Mosin, O.V. (2012) Isotopic Composition of Water and its Temperature in Modeling of Primordial Hydrosphere Experiments, VIII Intern. Conference Perspectives of the Development of Science and Technique, *Biochemistry and Biophysics*, **15**: 41–49.

Ignatov, I. & Mosin, O. V. & Naneva, K. (2012) Water in the Human Body is Information Bearer about Longevity, *Euromedica*, Hanover: 110-111.

Ignatov, I. & Mosin, O. V. (2013) Method for Color Coronal (Kirlian) Spectral Analysis, *Biomedical Radio electronics, Biomedical Technologies and Radio electronics*, **3**: 38-47. [in Russian]

Ignatov I. & Mosin O.V. (2013) Possible Processes for Origin of Life and Living Matter with Modeling of

Physiological Processes of Bacterium *Bacillus Subtilis* in Heavy Water as Model System, *Journal of Natural Sciences Research*, **3** (9): 65-76.

Ignatov, I. & Mosin, O. V. (2013) Modeling of Possible Processes for Origin of Life and Living Matter in Hot Mineral and Seawater with Deuterium, *Journal of Environment and Earth Science*, **3**(14): 103-118.

Ignatov, I., Mosin, O. V. (2013) Structural Mathematical Models Describing Water Clusters, *Journal of Mathematical Theory and Modeling*, **3** (11): 72-87.

Ignatov, I. & Mosin, O.V. (2014) Photoreceptors in Visual Perception and Additive Color Mixing. Bacteriorhodopsin in Nano- and Biotechnologies, *Advances in Physics Theories and Applications*, **27**: 20-37.

Ignatov, I. & Mosin, O. V. (2014) The Structure and Composition of Carbonaceous Fullerene Containing Mineral Shungite and Microporous Crystalline Aluminosilicate Mineral Zeolite. Mathematical Model of Interaction of Shungite and Zeolite with Water Molecules *Advances in Physics Theories and Applications*, **28**: 10-21.

Ignatov, I., Mosin, O.V., Velikov, B., Bauer, E. & Tyminski, G. (2014) Longevity Factors and Mountain Water as a Factor. Research in Mountain and Field Areas in Bulgaria, *Civil and Environmental Research*, **6** (4): 51-60.

Ignatov, I., Mosin, O. V., Niggli, H. & Drossinakis, Ch. (2014) Evaluating Possible Methods and Approaches for Registering of Electromagnetic Waves Emitted from the Human Body, *Advances in Physics Theories and Applications*, **30**: 15-33.

Ignatov, I., Mosin, O.V. & Drossinakis, Ch. (2014) Infrared Thermal Field Emitted from Human Body. Thermovision, *Journal of Medicine, Physiology, Biophysics*, **1**: 1-12.

Ignatov, I., Mosin, O.V. & Velikov, B. (2014) Longevity Factors and Mountain Water of Bulgaria in Factorial Research of Longevity, *Journal of Medicine, Physiology, Biophysics*, **1**: 13-33.

Ignatov, I. & Mosin, O.V. (2014) Visual Perception. Electromagnetic Conception for the Eyesight. Rhodopsin and Bacteriodopsin, *Journal of Medicine, Physiology and Biophysics*, **2**: 1-19.

Ignatov, I. & Mosin, O.V. (2014) The Structure and Composition of Shungite and Zeolite. Mathematical Model of Distribution of Hydrogen Bonds of Water Molecules in Solution of Shungite and Zeolite, *Journal of Medicine, Physiology and Biophysics*, **2**: 20-36.

Ignatov, I., Mosin, O.V., Velikov, B., Bauer, E. & Tyminski, G. (2014) Research of Longevity Factors and Mountain Water as a Factor in Teteven Municipality, Bulgaria, *Journal of Medicine, Physiology and Biophysics*, **2**: 37-52.

Ignatov, I. & Mosin, O.V. (2014) Modeling of Possible Processes for Origin of Life and Living Matter in Hot Mineral Water. Research of Physiological Processes of Bacterium *Bacillus Subtilis* in Hot Heavy Water, *Journal of Medicine, Physiology and Biophysics*, **2**: 53-70.

Ignatov, I. & Mosin, O.V. (2014) Mathematical Models of Distribution of Water Molecules Regarding Energies of Hydrogen Bonds, *Journal of Medicine, Physiology and Biophysics*, **2**: 71-94.

Ignatov, I. & Mosin, O.V. (2014) Modeling of Possible Conditions For Origin of First Organic Forms in Hot Mineral Water, *Journal of Medicine, Physiology and Biophysics*, **3**: 1-14.

Ignatov, I. & Mosin, O.V. (2014) Mathematical Model of Interaction of Carbonaceous Fullerene Containing Mineral Shungite and Aluminosilicate Mineral Zeolite with Water, *Journal of Medicine, Physiology and Biophysics*, **3**: 15-29.



Ignatov, I. & Mosin, O.V. (2014) Studying of Phototransformans of Light Signal by Photoreceptor Pigments – Rhodopsin, Iodopsin and Bacteriorhopsin and Additive Mixing of Colors, *Journal of Medicine, Physiology and Biophysics*, **3**: 30-47.

Ignatov, I. & Mosin, O.V. (2014) Mathematical Models Describing Water Clusters as Interaction among Water Molecules. Distributions of Energies of Hydrogen Bonds, *Journal of Medicine, Physiology and Biophysics*, **3**: 48-70.

Ignatov, I., Mosin, O. V. & Bauer, E. (2014) Carbonaceous Fullerene Mineral Shungite and Aluminosilicate Mineral Zeolite. Mathematical Model and Practical Application of Water Solution of Water Shungite and Zeolite, *Journal of Medicine, Physiology and Biophysics*, **4**: 27-44.

Ignatov, I. & Mosin, O. V. (2014) Nature of Hydrogen Bonds in Liquids and Crystals. Ice Crystal Modifications and Their Physical Characteristics, *Journal of Medicine, Physiology and Biophysics*, **4**: 58-80.

Ignatov, I. & Mosin, O. V. (2014) Research of Isotopic Effects of Deuterium in Cells of Microorganisms in the Presence of D<sub>2</sub>O in IR Spectra in Hot Mineral Water for Origin of Life, *Journal of Medicine, Physiology and Biophysics*, **4**: 45-57.

Ignatov, I. & Mosin, O. V. (2014) Visual Perception and Electromagnetic Conception for the Eyesight. Rhodopsin and Bacteriorhodopsin in Nano- and Biotechnologies, *Journal of Health, Medicine and Nursing*, **4**: 1-20.

Ignatov, I., Mosin, O.V., Velikov, B., Bauer, E. & Tyminski, G. (2014) Research of Longevity Factors and Mountain Water as a Factor in Teteven, Yablanitsa and Ugarchin Municipalities, Lovech Region, Bulgaria, *Journal of Health, Medicine and Nursing*, **4**: 21-36.

Ignatov, I. Mosin, O.V., Velikov, B. Bauer, E. & Tyminski, G. (2014) Mountain Water as Main Longevity Factor in Research of Phenomenon of Longevity in Mountain Areas in Bulgaria, *European Journal of Molecular Biotechnology*, **4** (2): 52-71.

Ignatov, I., Mosin, O. V., Niggli, H., Drossinakis, Ch. & Stoyanov, Ch. (2014) Registration of Electromagnetic Waves Emitted the Human Body, *Journal of Medicine, Physiology and Biophysics*, **5**: 1-22.

Ignatov, I. & Mosin, O. V. (2014) Modeling of Possible Processes for Origin of Life and Living Matter in Sea and Hot Mineral Water. Process of Formation of Stromatolites, *Journal of Medicine, Physiology and Biophysics*, **5**: 23-46.

Ignatov, I., Mosin, O. V. (2014) Coronal Gas Discharge Effect in Modeling of Non-Equilibrium Conditions with Gas Electric Discharge Simulating Primary Atmosphere and Hydrosphere for Origin of Life and Living Matter, *Journal of Medicine, Physiology and Biophysics*, **5**: 47-70.

Ignatov, I., Mosin, O. V. & Bauer, E. (2014) Mathematical Model and Practical Application of Water Solution of Shungite and Zeolite. Composition of Aluminosilicate Mineral Zeolite and Carbonaceous Fullerene Containing Mineral Shungite, *Journal of Health, Medicine and Nursing*, **5**: 12-29.

Ignatov, I. & Mosin, O. V. (2014) Hydrogen Bonds among Molecules in Liquid and Solid State of Water. Modifications of Ice Crystals, *Journal of Health, Medicine and Nursing*, **5**: 56-79.

Ignatov, I. & Mosin, O. V. (2014) Microorganisms in the Presence of D<sub>2</sub>O and IR Spectra in Hot Mineral Water with More Deuterium Atoms for Origin of Life and Living Matter, *Journal of Health, Medicine and Nursing*, **5**: 80-93.

- Ignatov, I. & Mosin, O.V. (2014) Color Coronal (Kirlian) Spectral Analysis in Modeling of Nonequilibrium Conditions with the Gas Electric Discharges, Simulating Primary Atmosphere, *Biomedical Radioelectronics*, **2**: 42-51. [in Russian]
- Ignatov, I., Mosin, O.V. & Stoyanov, Ch. (2014) Biophysical Fields. Color Coronal Spectral Analysis. Registration with Water Spectral Analysis. Biophoton Emission, *Journal of Medicine, Physiology and Biophysics*, **6**: 1-22.
- Ignatov, I. & Mosin, O.V. (2014) Hot Mineral Water with More Deuterium for Origin of Live and Living Matter. Process of Formation of Stromatolites, *Journal of Health, Medicine and Nursing*, **6**: 1-24.
- Ignatov, I. & Mosin, O.V. (2014) Origin of Life and Living Matter in Primary Atmosphere and Hydrosphere. Modeling of Non-equilibrium Electric Gas Discharge Conditions, *Journal of Health, Medicine and Nursing* **6**: 25-49
- Ignatov, I. & Mosin, O.V. (2014) Methods for Measurements of Water Spectrum. Differential Non-equilibrium Energy Spectrum Method (DNES), *Journal of Health, Medicine and Nursing* **6**: 50-72.
- Karnaukhova, E.N., Mosin, O.V. & Reshetova, O.S. (1993) Biosynthetic production of stable isotope labeled amino acids using methylotroph *Methylobacillus flagellatum*. *Amino Acids*, **5**(1): 125.
- Karadzov, S., Atanasov, A., Ivanova, E., Mosin, O. V. & Ignatov, I. (2014) Mathematical Models of Electrochemical Aqueous Sodium Chloride Solutions (Anolyte and Catolyte) as Types of Water. Study of the Effects of Anolyte on the Virus of Classical Swine Fever Virus, *Journal of Health, Medicine and Nursing*, **5**: 30-55.
- Jushkin, N.P. (1994) Globular supramolecular structure shungite: data scanning tunneling microscopy. *Reports. Acad. Science USSR*, **337**(6), 800–803 [in Russian].
- Kasatochkin, V.I., Elizen, V.M., Melnichenko, V.M., Yurkovsky, I.M. & Samoilov, V.S. (1978) Submikroporous structure of shungites. *Solid Fuel Chemistry*, **3**, 17–21.
- Khadartsev, A.A. & Tuktamyshev, I.S. (2002) Shungites in medical technologies. *Vestnik Novih Medicinskih Technologii*, **9**(2): 83-86 [in Russian].
- Kovalevski, V.V. (1994) Structure of shungite carbon. *Natural Graphitization Chemistry*, **39**, 28–32.
- Kovalevski, V.V., Buseck, P.R. & Cowley J.M. (2001). Comparison of carbon in shungite rocks to other natural carbons: an X-ray and TEM study. *Carbon*, **39**: 243–256.
- Luck, W., Schiöberg, D. & Ulrich, S. (1980) Infrared investigation of water structure in desalination membranes. *J. Chem. Soc. Faraday Trans.*, **2**(76): 136–147.
- Mosin, O.V., Skladnev, D.A., & Shvets, V.I. (1998) Biosynthesis of <sup>2</sup>H-labeled Phenylalanine by a New Methylotrophic Mutant *Brevibacterium methylicum*, *Biosci Biotechnol Biochem.*, **62**(2):225–229.
- Mosin, O.V., Skladnev, D.A., & Shvets, V.I. (1999) Biosynthesis of <sup>2</sup>H-labelled Inosine by Bacterium *Bacillus subtilis*, *Izv. RAN. Ser. biologicheskaja.*, **4**:396–402 [in Russian].
- Mosin, O.V., Skladnev, D.A., & Shvets, V.I. (2000) Studying of Adaptation to Heavy Water, *Biotechnologija*, **10**:16–23 [in Russian].
- Mosin, O.V. & Ignatov I. (2012) Isotope Effects of Deuterium in Bacterial and Microalgae Cells at Growth on Heavy Water (D<sub>2</sub>O), *Water: Chemistry and Ecology*, **3**:83–94 [in Russian].
- Mosin, O.V., Shvets, V.I., Skladnev, D.A., & Ignatov, I. (2012) Studying of Microbic Synthesis of Deuterium Labeled L-phenylalanine by Methylotrophic Bacterium *Brevibacterium Methylicum* on Media with Different Content of Heavy Water, *Russian Journal of Biopharmaceuticals*, **4** (1): 11–22 [in

Russian].

Mosin, O.V., & I. Ignatov, I. (2013) Microbiological Synthesis of  $^2\text{H}$ -labeled Phenylalanine, Alanine, Valine, and Leucine/isoleucine with Different Degrees of Deuterium Enrichment by the Gram-positive Facultative Methylotrophic Bacterium *Brevibacterium methylicum*, *International Journal of BioMedicine*, **3**(2): 132–138.

Mosin, O.V., Shvets, V.I., Skladnev, D.A., & Ignatov, I. (2013) Microbiological synthesis of [ $^2\text{H}$ ]inosine with high degree of isotopic enrichment by Gram-positive chemoheterotrophic bacterium *Bacillus subtilis*, *Applied Biochemistry and Microbiology*, **49** (3): 255–266.

Mosin, O. V, Ignatov, I. (2012) Studying of Isotopic Effects of Heavy Water in Biological Systems on Example of Prokaryotic and Eukaryotic Cells, *Biomedicine*. **1** (1-3): 31-50.

Mosin, O. V.& I. Ignatov, I. (2013b) The Structure and Composition of Natural Carbonaceous Fullerene Containing Mineral Shungite, *International Journal of Advanced Scientific and Technical Research*, **3**, **6**(11-12): 9-21.

Mosin, O. V., Ignatov, I., Skladnev, D. A & Shvets, V. I. (2013) Use of Gram-positive Chemoheterotrophic Bacterium *Bacillus Subtilis* B-3157 with HNP-cycle of Carbon Assimilation for Microbiological Synthesis of [ $^2\text{H}$ ] riboxine with High Level of Deuterium Enrichment, *European Journal of Molecular Biotechnology*, **2**: 63-78.

Mosin, O. V., Shvets, V. I, Skladnev, D. A. & Ignatov, I. (2013) Microbiological Synthesis of [ $^2\text{H}$ ]-inosine with High Degree of Isotopic Enrichment by Gram-positive Chemoheterotrophic Bacterium *Bacillus Subtilis*, *Applied Biochemistry and Microbiology*, **49** (3): 233-243.

Mosin, O.V. & Ignatov, I (2014) Biosynthesis of photochrome transmembrane protein bacteriorhodopsin of *Halobacterium halobium* labeled with deuterium at aromatic amino acids residues of [2,3,4,5,6- $^2\text{H}_5$ ]Phe, [3,5- $^2\text{H}_2$ ]Tyr and [2,4,5,6,7 - $^2\text{H}_5$ ]Trp. *Chemistry and Materials Research*, **6**(3): 38-48.

Mosin, O. V., Shvets, V. I, Skladnev, D. A. & Ignatov, I. (2013) Microbial Synthesis of  $^2\text{H}$ -labelled L-phenylalanine with Different Levels in Isotopic Enrichment by a Facultative Methylotrophic *Brevibacterium Methylicum* with RuMP Assimilation of Carbon, *Supplement Series B: Biomedical Chemistry*, **7** (3): 247-258.

Mosin, O.V. & Ignatov, I. (2013) Studying of the biosynthesis of  $^2\text{H}$ -labeled inosine by a Gram-positive chemoheterotrophic bacterium *Bacillus subtilis* B-3157 on heavy water ( $^2\text{H}_2\text{O}$ ) medium. *Chemical and Process Engineering Research*, **15**: 32–45.

Mosin, O.V., Shvets, V.I., Skladnev, D.I. & Ignatov, I (2013) Microbial synthesis of  $^2\text{H}$ -labelled L-phenylalanine with different levels of isotopic enrichment by a facultative methylotrophic bacterium *Brevibacterium methylicum* with RuMP assimilation of carbon. *Biochemistry (Moscow) Supplement Series B:Biomedical Chemistry*, **7**(3): 249-260 .

Mosin, O.V., Ignatov, I., Skladnev, D. A.&Shvets, V.I. (2014) Using of Facultative Methylotrophic Bacterium *Brevibacterium Methylicum* B-5652 with RMP-cycle of Carbon Assimilation for Microbiological Synthesis of [ $^2\text{H}$ ] phenylalanine with Different Levels of Deuterium Enrichment, *European Journal of Molecular Biotechnology*, **3**(1):25-40.

Mosin,O.V.&Ignatov, I. (2014) Biological Influence of Deuterium on Prokaryotic and Eukaryotic Cells, *European Journal of Molecular Biotechnology*, **3**(1):11-24.

Mosin, O.V.&Ignatov, I. (2014) Preparation of Highly Deuterated Phenylalanine, Alanine, Valine, and

- Leucine/Isoleucine Using Facultative Methylophilic Bacterium *Brevibacterium Methylicum*, *Journal of Medicine, Physiology, Biophysics*, **1**:34-51.
- Mosin, O.V.&Ignatov, I. (2014) Biological Influence of Deuterium on Prokaryotic and Eukaryotic cells, *Journal of Medicine, Physiology, Biophysics*, **1**: 52-72.
- Mosin, O.V.&Ignatov, I. (2014) Studying Biosynthetic Pathways of <sup>2</sup>H-Labeled Purine Ribonucleoside Inosine in a Bacterium *Bacillus Subtilis* B-3157 by FAB Method, *Journal of Medicine, Physiology, Biophysics*, **1**:73-90.
- Mosin, O.V.&Ignatov, I. (2014) Basic Concept of Magnetic Water Treatment, *European Journal of Molecular Biotechnology*, **4** (2): 72-85.
- Paton, D.J.&I. Greiser-Wilke (2003): Classical swine fever – an update, *Res.inVet.Sci.*, **75**: 169-178.
- Parfen'eva, L.S. (1994) Electrical conductivity of shungite carbon. *Solid State Physics*, **36**(1), 234–236.
- Podchaynov, S.F. (2007) Mineral zeolite – a multiplier of useful properties shungite. Shungites and human safety, in *Proceedings of the First All-Russian scientific-practical conference* (3–5 October 2006), ed. J.K Kalinin (Petrozavodsk: Karelian Research Centre of Russian Academy of Sciences), 6–74 [in Russian].
- Reznikov, V.A. & Polehovskiy, Y.S. (2000) Shungite amorphous carbon – the natural environment of fullerene. *Technical Physics Letters*, **26**(15), 689–693.
- Sands, J.A., Landin, P.&Auperin, D. (1979) Enveloped virus inactivation by fatty acid derivatives“, *Antimicrob.Agents Chemother.*, **15**: 134-136.
- Springthorpe, U.S., Sattar, S.A. (1990) Chemical disinfection of virus- contaminated surfaces. *Crit.Rev.Environ.Control*, **20**: 169-229
- Van Den Bossche&G., Strauch, D. (1991): Zur Wirksamkeit von Flächendesinfektionsmitteln und ihrem Einsatz in der Tierhaltung“. *BL- Journal*, **1**: 110-126.